



# A *GALEX* far-ultraviolet study of quasi-coeval samples of red giants

Graeme H. Smith<sup>1</sup> · Kevin M. Cochrane<sup>2</sup>

Received: 5 September 2019 / Accepted: 23 May 2020 / Published online: 3 June 2020  
© Springer Nature B.V. 2020

**Abstract** Samples of red giant branch (RGB) stars have been compiled from the literature for seven moving groups, and searches made for both *GALEX* FUV and Johnson *BV* photometry. It has been possible to derive a colour index ( $FUV - B$ ) for many giants, which has been combined with  $B - V$  to give a two-colour diagram for each kinematic group. In addition, analogous data have been gleaned for a small number of red giants in the open cluster NGC 752.

Optical photometry has been combined with parallax and proper motion data from the *Gaia* DR2 data release to document the colour-magnitude diagram (CMD) positions and space motion velocities among the proposed group giants. Comparisons with isochrones confirm a range in age among the groups considered. However, none of the group samples evince RGB sequences as tight in the CMD as those typical of open clusters. Considering also the velocity dispersions found within each set of group candidates, it is concluded that the fraction of non-members included may be significant.

The RGB stars ascribed to different moving groups are largely located within overlapping regions of the FUV two-colour diagram, without any obvious systematic offsets between groups of different age. All of the RGB sequences attain a maximum ( $FUV - B$ ) colour of  $\approx 14.2$ – $14.5$  mag within the optical colour range of  $1.0 < B - V < 1.25$ . Many of the stars in this range are in the core-helium-burning (CHB) phase of evolution. On the red side of the

CHB region in the two-colour diagram, i.e., at  $B - V > 1.25$ , the RGB stars from different groups largely map out a common locus.

Among CHB and other giants blueward of  $B - V = 1.25$  there are a number of stars with FUV-excesses ranging from 2–4 mag as judged by the ( $FUV - B$ ) colour. There is found evidence for a range in chromospheric activity among CHB stars. By analogy with known properties of Hyades cluster giants a range in activity among the CHB stars within a moving group may be a consequence of different degrees of spindown corresponding to different amounts of time spent in the core-helium-burning phase.

**Keywords** Stars: activity · Ultraviolet: stars

## 1 Introduction

The far-ultraviolet (FUV) spectrum of late-F, G and K stars provides a gateway to conditions in the chromospheres and transition regions of these stars (e.g., Redfield et al. 2002; Dupree et al. 2005; Ayres 2015). As a by-product of the large-sky imaging survey made by the *GALEX* satellite observatory (Martin et al. 2005; Bianchi 2014) there is available a rich data set of stellar broadband photometry in the wavelength range 1350–1750 Å, the so-called *GALEX* FUV channel. Studies of FGK *dwarfs* have shown that the *GALEX* FUV magnitude correlates with other indicators of the level of surface activity of these stars, such as Ca II H and K line emission and coronal soft x-ray emission (e.g., Smith and Redenbaugh 2010; Findeisen et al. 2011; Smith et al. 2017; Richey-Yowell et al. 2019). Studies of M *dwarfs* have also shown that *GALEX* FUV data can yield a valuable stellar activity tracer (Shkolnik and Barman 2014) for even

✉ G.H. Smith  
graeme@ucolick.org

K.M. Cochrane  
kmcochra@ucsc.edu

<sup>1</sup> University of California Observatories/Lick Observatory,  
University of California, Santa Cruz, CA 95064, USA

<sup>2</sup> Department of Physics, University of California, Santa Cruz, CA  
95064, USA

cooler spectral types. Although *giant* stars of FGK spectral type are also known to have chromospheres and varying degrees of coronal activity (e.g., Wilson 1982; Rutten 1987; Dupree et al. 1990, 1999; Judge and Stencel 1991; Pasquini et al. 1990; Pasquini and Brocato 1992; Strassmeier 1994; Schröder et al. 2018) the *GALEX* FUV characteristics of this luminosity class have not been as extensively studied as for dwarfs.

Smith (2018, 2019) studied the *GALEX* FUV properties of a set of field red giants and showed that the relative strength of FUV flux does correlate with the level of chromospheric activity as traced by the Mg II *h* and *k* emission lines. The field sample considered by Smith (2018), which is based upon a study of IUE spectra by Pérez Martínez et al. (2011), is likely quite inhomogeneous as regards age, a stellar property which can be influential in setting the level of chromospheric and coronal activity of a star.

Open clusters can offer chemically homogeneous systems of coeval red giants. However, few of the open clusters with any significant number of red giants were amenable to deep imaging observation by the *GALEX* observatory. A second albeit less precise way of obtaining samples of potentially coeval red giants is to draw them from catalogued members of a kinematically-defined moving group (Eggen 1965a, 1996). A moving group is identified among field stars having nearly identical space velocities. Similar kinematics may indicate that the stars of a given group formed together within a cluster or association that since became unbound (e.g., Asiain et al. 1999). Metallicity and chemical abundance properties of kinematically-selected stars can provide additional tests for group membership. Studies such as Boyle and McClure (1975), De Silva et al. (2007, 2011), Liu et al. (2012), and Taberner et al. (2017), have tended to reveal chemically homogeneous subsets of stars within kinematically chosen samples from groups such as the HR 1614 system, although the degree of chemical inhomogeneity does vary. On this basis, reservoirs for studying the FUV properties of “quasi-coeval” red giants can be sought by selecting stars for which there is prior indication of membership of a moving group.

The aim of this paper is to present *GALEX* FUV photometry for samples of red giants that have been associated with seven different moving groups, as well as the open cluster NGC 752. By contrast, studies of FUV activity among dwarf stars in moving groups have been made by Findeisen et al. (2011), Murgas et al. (2013), Rodriguez et al. (2013), Richey-Yowell et al. (2019), and Cochrane and Smith (2019). The red giants in the present study have been selected from the Hyades, Wolf 630, Ursa Major, HR 1614,  $\zeta$  Herculis,  $\sigma$  Puppis, and  $\eta$  Cephei moving groups.

## 2 Literature sources for giant stars in moving groups

Various literature sources were used to compile lists of giant stars which have been identified as possible members of moving groups. This section describes the kinematic groups that have been considered, and provides references to the papers from which initial lists of candidate-member stars were derived.

One of the first moving groups to have been identified is kinematically associated with the Hyades open cluster (Proctor 1869). Quite a few red giant stars have been connected to the Hyades moving group. The sources from which the red giants listed in Table 1 were drawn are the papers of Eggen (1985a, 1985b, 1985c) and Boyle and McClure (1975). The age and metallicity of the Hyades moving group is presumed to be identical to those of the Hyades cluster, for which Perryman et al. (1998) give 0.63 Gyr and  $[\text{Fe}/\text{H}] = +0.14$  respectively. However, Ramya et al. (2019) found a range in abundance of  $-0.20 \leq [\text{Fe}/\text{H}] \leq +0.25$  among red giants in the Hyades “supercluster,” and concluded that few if any of the giants in this kinematic system originated from a common open cluster.

Another moving group for which a relatively large number of red giant members has been proposed is that associated with the star Wolf 630 (Eggen 1965b). Papers by McDonald and Hearnshaw (1983) and Bubar and King (2010) were used to draw up a list (Table 2) of red giants that are potentially members of this group. The Wolf 630 group was studied spectroscopically by Bubar and King (2010) who found a metallicity of  $[\text{Fe}/\text{H}] = -0.01$  and an age of 2.7 Gyr. This group appears therefore to be composed of stars some 2 Gyr older than those of the Hyades group.

One kinematic group that is associated with stars in Ursa Major (Proctor 1869) has been referred to by a variety of names including the Ursa Major moving group and the Sirius supercluster. Soderblom and Mayor (1993a) and King et al. (2003) carried out membership-likelihood studies of stars potentially affiliated with this group, and it is from their work that the giants listed in Table 3 were drawn. Bond et al. (2017) found an age of 0.24 Gyr for the star Sirius A, which may set an age for the Ursa Major group. Soderblom and Mayor (1993a, 1993b) state that the traditional age of the Ursa Major group is 0.3 Gyr, which they consider to be consistent with the rotation rates and levels of activity of main sequence stars assigned to the group. By contrast, King et al. (2003) found an isochrone age of  $0.5 \pm 0.1$  Gyr from an H-R diagram of group members. Although there is a range of some 0.2 Gyr in the age thereby inferred for the Ursa Major group, all estimates indicate it to be the youngest kinematic group in our sample. Red giants that have been associated with the Sirius supercluster were found by Ramya et al. (2019) to have a range in metallicity,

**Table 1** Candidate giant stars of the Hyades moving group

Star	$\pi$ (mas)	$V$	$(B - V)$	$M_V$	$(FUV - B)$	$U$ (km s <sup>-1</sup> )	$V$ (km s <sup>-1</sup> )	$W$ (km s <sup>-1</sup> )	$E(G_{BP} - G_{RP})$	Notes
HD 1014	7.843	5.128	1.577	-0.400	12.017	-33.0	-11.9	-3.5	0.37	V <sup>a</sup>
HD 1367	8.875	6.178	0.936	0.919	13.915	-43.6	-23.8	+4.2	...	
HD 5848	11.562	4.226	1.207	-0.459	14.022	-32.7	-11.2	+1.3	0.15	
HD 10859	8.28	6.314	0.947	0.904	10.491	-33.7	-21.2	-4.1	...	
HD 12402	7.4805	6.563	1.007	0.933	13.527	-50.0	-24.7	+6.4	...	
HD 13818	7.5268	6.36	1.05	0.743	13.300	-35.8	-17.8	-23.4	0.01	
HD 15889	7.0016	6.295	1.017	0.521	11.875	-30.9	-23.1	-1.2	...	
HD 17459	7.3266	5.847	1.13	0.172	14.038	-45.6	-18.2	-30.3	0.13	
HD 19787	20.3349	4.345	1.033	0.886	14.253	-37.9	-19.4	+5.5	0.06	V <sup>a</sup>
HD 20234	2.3755	5.726	2.431	-2.395	12.068	-41.8	-22.9	-1.8	...	V <sup>a</sup>
HD 26703	8.6673	6.243	1.147	0.932	13.595	-40.9	-11.4	-19.9	0.04	
HD 40827	7.2866	6.34	1.10	0.653	14.557	-43.0	-12.4	0.0	0.05	
HD 71952	16.7113	6.258	1.01	2.373	13.800	-34.5	-12.8	+26.4	...	
HD 73171	6.5343	5.915	1.167	-0.009	14.064	-38.1	-14.9	+0.5	0.10	
HD 94247	5.7649	5.09	1.36	-1.106	13.826	-45.2	-23.7	-21.1	0.20	
HD 97989	7.5002	5.88	1.078	0.255	14.182	-45.5	-24.8	-15.3	0.15	
HD 99322	12.4409	5.224	0.998	0.698	13.457	-37.1	-18.3	-5.0	0.10	
HD 100006	9.6412	5.525	1.059	0.446	13.607	-43.0	-10.8	+12.8	0.06	
HD 101112	8.3763	6.186	1.071	0.801	13.255	-31.4	-15.2	+2.4	0.02	
HD 109217	7.0337	6.280	0.955	0.516	13.730	-30.5	-15.3	-2.0	...	
HD 116976	12.5871	4.754	1.091	0.254	14.226	-45.3	-15.8	+2.4	...	V <sup>a</sup>
HD 117287	4.4682	5.614	1.574	-1.135	12.902	-46.9	-19.3	+7.6	...	MV <sup>a</sup>
HD 120084	9.676	5.907	1.013	0.835	13.726	-32.7	-16.5	-16.3	0.07	
HD 120452	13.9184	4.971	1.061	0.689	13.962	-44.5	-11.8	-28.1	0.04	
HD 131530	9.881	5.804	0.982	0.778	13.812	-28.0	-15.9	-3.9	0.02	
HD 143209	9.3219	6.307	1.075	1.155	14.041	-39.9	-18.4	+9.1	0.14	
HD 144046	8.2952	6.075	0.96	0.669	12.610	-44.8	-16.2	-8.6	...	
HD 190252	6.8074	6.33	0.88	0.495	12.033	-46.0	-17.7	-11.9	...	
HD 202951	2.7415	5.961	1.648	-1.849	12.246	-61.5	-17.5	+3.4	...	V <sup>a</sup>
HD 217382	8.9232	4.726	1.417	-0.521	13.717	-49.5	-19.9	-11.6	0.15	
HD 220572	10.9839	5.605	1.064	0.809	13.881	-37.3	-15.7	+5.1	0.02	HB <sup>a</sup>
HD 222683	8.9046	6.29	0.96	1.038	13.223	-44.6	-17.5	-7.1	...	

<sup>a</sup>HB: core-helium-burning star; LPV: long period variable; MV: Mira variable; V: other type of variable star

$-0.22 \leq [\text{Fe}/\text{H}] \leq +0.15$ , and they concluded that these giants also did not originate from a single cluster. Evidence such as this has been used to infer a non-common origin for the giants in the Hyades and Ursa Major groups, with dynamical effects induced by a non-axisymmetric Galaxy being one hypothesis for the kinematic ordering of non-coeval stars (e.g., Famaey et al. 2008). Dopcke et al. (2019) derived abundances for a wide variety of elements for candidate dwarf stars in the Ursa Major group. They found that a fraction (albeit small) of these stars do constitute a chemically homogeneous set with a metallicity near solar.

The HR 1614 moving group was identified by Eggen (1978), and is noteworthy for some relatively metal-rich

abundance patterns among its stars (Eggen 1978, 1998; Smith 1983; Feltzing and Holmberg 2000; De Silva et al. 2007). The age derived for the group has differed between authors, ranging from  $\sim 2$  Gyr (Feltzing and Holmberg 2000; De Silva et al. 2007) to  $\sim 4$  Gyr (Eggen 1998; Barnes 2007), while spectroscopy has revealed a system with metallicity even higher than that of the Hyades ( $[\text{Fe}/\text{H}] = +0.25$ ; De Silva et al. 2007). The HR 1614 system is one moving group whose kinematics and metallicity patterns are consistent with an origin in a unique but now disrupted cluster (De Silva et al. 2007). Table 4 gives a listing of proposed group giants as drawn from Eggen (1996, 1998) and Feltzing and Holmberg (2000).

**Table 2** Candidate giant stars of the Wolf 630 moving group

Star	$\pi$ (mas)	$V$	$(B - V)$	$M_V$	$(FUV - B)$	$U$ (km s <sup>-1</sup> )	$V$ (km s <sup>-1</sup> )	$W$ (km s <sup>-1</sup> )	$E(G_{BP} - G_{RP})$	Notes
HD 1038	6.9100	4.431	1.648	-1.255	11.980	+39.0	-38.7	+17.3	...	LPV
HD 2806	3.9374	6.86	1.21	-0.081	12.924	+26.4	-30.9	-29.0	0.12	
HD 4188	14.4124	4.755	1.013	0.479	13.912	+21.9	-28.4	-10.4	0.15	V
HD 4928	8.5500	6.364	1.070	0.159	14.051	+3.9	-29.5	-28.6	0.08	
HD 5384	5.5744	5.850	1.522	-0.480	13.278	+23.7	-25.1	-18.0	0.17	
HD 8498	4.4877	5.840	1.608	-1.541	12.350	+43.0	-26.3	+22.0	0.27	V
HD 8763	10.6874	5.494	1.106	0.833	14.203	+12.3	-51.3	+13.4	0.08	
HD 14728	8.0080	5.872	1.225	0.209	14.200	+17.4	-29.8	-6.8	0.20	
HD 15652	5.2608	6.127	1.578	0.103	13.099	+23.3	-19.6	+18.4	0.38	
HD 15656	7.1563	5.156	1.470	-0.460	13.078	+0.9	-36.4	+33.1	0.26	
HD 16060	8.4789	6.183	1.053	0.804	14.154	+47.5	-51.4	-16.3	0.02	
HD 17017	8.5941	6.40	1.04	1.325	14.029	+17.8	-37.4	+15.8	0.09	
HD 17491	3.6140	6.815	1.586	-0.230	11.490	+46.1	-42.7	-8.2	...	LPV
HD 17829	6.8433	5.474	1.254	-0.270	13.897	+23.9	-31.2	-8.0	0.15	
HD 18322	25.2039	3.886	1.104	0.777	14.027	+2.1	-42.4	-26.9	0.08	V
HD 24706	9.4947	5.928	1.239	0.768	14.193	+9.0	-15.2	+7.5	0.13	
HD 25069	21.2353	5.833	1.000	2.498	14.236	-2.5	-29.6	-47.3	...	
HD 26967	27.9235	3.854	1.098	1.118	14.131	+22.7	-33.4	-9.2	0.13	
HD 27588	13.4050	5.332	1.078	0.892	13.964	-1.3	-35.6	-1.0	0.03	
HD 30959	6.1623	4.720	1.789	-1.781	9.407	+19.4	-32.4	-22.2	...	LPV
HD 39523	18.5626	4.500	1.100	0.830	12.578	+17.8	-27.1	+8.1	0.03	
HD 41698	4.3670	6.879	1.595	0.339	11.055	+5.7	-18.9	-4.9	...	LPV
HD 49878	17.1931	4.542	1.365	0.788	13.846	+22.6	-28.2	+4.3	0.22	
HD 54131	11.2090	5.457	1.020	0.481	13.855	+26.9	-31.1	-23.4	0.03	
HD 55383	5.5716	5.067	1.653	-1.031	11.179	+20.6	-32.5	-6.8	...	LPV
HD 60522	12.3525	4.058	1.540	-0.539	13.066	+17.8	-31.2	-32.6	...	V
HD 82870	6.4053	5.557	1.160	-0.641	14.001	+21.9	-37.5	-9.8	0.12	
HD 83618	13.5761	3.900	1.320	-0.635	13.708	+11.5	-30.7	+14.6	...	V
HD 84542	2.7225	5.804	1.635	-3.095	12.372	+23.9	-32.0	-11.3	0.48	V
HD 85945	7.3538	5.944	0.890	0.129	11.222	+41.8	-48.6	-9.8	...	
HD 89962	13.4045	6.055	1.120	1.795	13.955	+20.7	-15.2	-35.9	0.15	
HD 92620	4.0122	5.997	1.617	-0.982	11.574	-0.8	-24.1	+12.5	...	LPV
HD 94237	3.8957	6.303	1.500	-0.891	13.663	+7.2	-28.4	-9.5	0.28	
HD 94264	31.2707	3.816	1.038	1.498	13.984	+17.7	-38.0	+22.9	0.20	V
HD 94669	10.0490	6.034	1.128	1.134	13.791	+42.5	-45.0	-37.9	0.04	
HD 97605	15.2500	5.788	1.118	1.877	13.945	+24.7	-29.9	+8.1	0.24	
HD 99592	3.9069	6.191	1.684	-3.110	10.460	+2.8	-25.1	-16.7	...	LPV
HD 105639	13.4275	5.938	1.120	1.620	13.912	+43.8	-42.3	-23.4	...	
HD 110418	3.5519	6.78	1.58	-0.204	12.325	+43.5	-30.1	-36.1	...	
HD 117267	6.5986	6.422	1.117	0.394	14.143	+10.7	-61.3	+17.1	0.13	
HD 124679	11.8437	5.287	1.004	0.738	13.367	+39.7	-55.6	-2.2	0.09	
HD 136366	5.8876	6.164	1.023	-0.154	13.839	+16.0	-40.5	-25.4	...	
HD 137613	0.8999	7.484	1.186	-1.389	9.247	+51.2	-49.0	-1.3	...	V
HD 142091	33.2328	4.812	0.996	2.391	13.931	+32.7	-40.9	-18.8	...	
HD 144542	3.2226	6.189	1.576	-1.160	12.522	+31.2	-32.1	+29.7	0.44	V
HD 148513	7.3867	5.384	1.458	-0.098	13.510	+28.6	-28.8	-17.8	0.16	
HD 156074	3.4590	7.602	1.147	0.335	12.497	+47.8	-32.2	-5.8	...	
HD 188887	13.8248	5.307	1.220	1.006	13.159	+13.1	-37.3	-31.2	0.10	
HD 197635	10.0693	5.411	1.120	0.578	14.066	+22.0	-31.2	+18.4	0.21	HB
HD 197964	28.5183	3.906	0.847	0.966	10.480	+21.2	-22.6	-12.7	...	
HD 202573	5.8960	6.969	0.890	0.566	13.510	+50.1	-34.9	+25.8	...	
HD 203638	12.9065	5.355	1.160	1.027	13.922	+29.3	-35.7	-24.0	0.05	V
HD 210066	7.1245	4.983	1.492	-0.587	10.818	+15.5	-29.7	-18.4	0.24	
HD 215104	14.4687	4.839	1.027	0.594	13.702	+19.2	-31.4	-23.4	0.15	
HD 217701	3.6764	6.133	1.589	-2.116	13.113	+27.4	-34.2	-9.0	0.49	V

**Table 3** Candidate giant stars of the Ursa Major moving group

Star	$\pi$ (mas)	$V$	$(B - V)$	$M_V$	$(FUV - B)$	$U$ (km s <sup>-1</sup> )	$V$ (km s <sup>-1</sup> )	$W$ (km s <sup>-1</sup> )	$E(G_{BP} - G_{RP})$	Notes
HD 745	8.2353	7.45	0.90	2.028	12.873	+21.7	+0.7	-1.5	...	
HD 2410	6.7697	6.38	1.00	0.533	13.787	+16.2	+4.7	-11.7	...	
HD 16161	8.5202	4.97	0.87	-0.378	12.824	+13.6	-0.5	-16.3	...	
HD 18645	6.0491	7.86	0.75	1.768	10.195	+14.5	-10.0	-8.5	1.11	V
HD 30834	6.334	4.781	1.415	-1.211	13.526	+20.3	+5.6	-15.3	0.21	
HD 99648	6.3284	4.953	1.003	-1.041	13.626	+15.6	+2.5	-7.1	...	
HD 152863	8.2722	6.081	0.921	0.669	14.372	+11.0	+0.1	-10.8	...	
HD 199951	14.6428	4.669	0.890	0.497	11.719	+15.9	-1.6	-9.2	...	
HD 210459	13.0102	4.291	0.461	-0.138	9.136	+8.1	+3.5	-4.7	...	
HD 220096	9.7465	5.650	0.814	0.594	10.086	+14.9	+0.9	-12.6	...	

**Table 4** Candidate giant stars of the HR 1614 moving group

Star	$\pi$ (mas)	$V$	$(B - V)$	$M_V$	$(FUV - B)$	$U$ (km s <sup>-1</sup> )	$V$ (km s <sup>-1</sup> )	$W$ (km s <sup>-1</sup> )	$E(G_{BP} - G_{RP})$	Notes
HD 2140	4.4097	6.78	1.30	0.002	13.375	-6.9	-65.8	-17.4	0.07	
HD 28479	11.0099	5.958	1.215	1.167	14.478	+14.5	-52.9	-18.1	0.13	
HD 33042	7.8033	5.028	1.502	-0.511	13.307	-12.1	-53.0	+11.0	0.28	V
HD 38358	6.2852	6.29	1.35	0.282	13.944	+5.7	-61.9	-31.5	0.14	
HD 40176	10.0920	4.973	1.105	-0.007	11.709	-13.4	-60.3	-13.8	...	
HD 65953	7.5710	4.676	1.491	-0.928	13.165	+25.1	-60.3	+20.8	0.16	
HD 114092	7.0054	6.188	1.361	0.415	13.697	+1.8	-50.6	-10.4	0.13	
HD 115467	6.8736	6.68	1.07	0.866	13.717	+7.9	-53.3	-6.9	0.02	
HD 117267	6.5986	6.422	1.117	0.519	14.143	+10.7	-61.3	+17.1	0.13	
HD 141477	9.9009	4.097	1.612	-0.925	12.421	-3.5	-57.6	-23.1	...	V
HD 146388	10.6571	5.701	1.126	0.839	13.879	+5.0	-51.9	-1.4	0.02	
HD 219263	13.9169	5.776	1.166	1.494	13.691	-20.4	-48.4	-9.5	0.21	

**Table 5** Candidate giant stars of the  $\zeta$  Herculis moving group

Star	$\pi$ (mas)	$V$	$(B - V)$	$M_V$	$(FUV - B)$	$U$ (km s <sup>-1</sup> )	$V$ (km s <sup>-1</sup> )	$W$ (km s <sup>-1</sup> )	$E(G_{BP} - G_{RP})$	Notes
HD 1187	7.4651	5.662	1.350	0.027	13.617	-53.4	-50.1	-35.3	0.10	
HD 12274	10.7786	3.992	1.572	-0.845	12.818	-40.3	-47.5	-3.3	...	
HD 13596	6.0939	5.703	1.548	-0.373	12.791	-62.2	-51.9	-2.7	0.24	V
HD 43899	11.6264	5.557	1.128	0.884	13.876	-60.9	-54.3	-19.4	0.03	
HD 90250	7.4691	6.474	1.095	0.840	14.147	-53.2	-51.5	-23.5	0.02	
HD 96813	7.7463	5.785	1.498	0.230	11.772	-27.5	-23.3	+11.5	...	LPV
HD 129245	6.5901	6.260	1.300	0.354	13.441	-77.2	-51.2	-30.2	0.16	

Three other less populous groups are included in the present study. The  $\zeta$  Herculis,  $\sigma$  Puppis, and  $\eta$  Cephei groups were identified by Eggen (1958, 1971), and it is from the second of these papers that the lists of red giants in Tables 5–7 were obtained. All three groups are older than the Hyades. Although Eggen (1971) considered these groups to be part of an old disk stellar population, more recent studies of the eponymous stars for two of them indicate ages

younger than the Sun. Affer et al. (2005) give an isochrone age of 2.5 Gyr for the star  $\eta$  Cephei (HD 198149) and measured a metallicity of  $[Fe/H] = -0.2 \pm 0.2$ . Morel et al. (2001) found an isochrone age of 3.4–3.6 Gyr for component A of the  $\zeta$  Herculis binary star, with a metallicity close to solar. The  $\sigma$  Pup group has received relatively little attention, with Wegner (1976) finding  $[Fe/H] = -0.5$  to  $-0.4$

**Table 6** Candidate giant stars of the  $\sigma$  Puppis moving group

Star	$\pi$ (mas)	$V$	$(B - V)$	$M_V$	$(FUV - B)$	$U$ (km s $^{-1}$ )	$V$ (km s $^{-1}$ )	$W$ (km s $^{-1}$ )	$E(G_{BP} - G_{RP})$	Notes
HD 2490	7.7594	5.424	1.559	-0.127	13.306	-54.4	-67.1	-34.5	0.28	
HD 3457	4.8860	6.391	1.342	-0.164	13.587	-49.8	-83.7	-4.2	0.20	
HD 37763	31.1021	5.176	1.130	2.640	14.288	-25.9	-65.6	-18.7	...	
HD 40801	13.8158	6.093	0.977	1.795	13.771	-42.1	-56.6	+19.3	...	
HD 77729	2.1477	7.629	1.402	-0.711	13.141	-94.8	-103.1	+10.1	0.25	
HD 100470	7.7104	6.387	1.056	0.822	14.199	-63.1	-57.9	+1.0	0.02	
HD 124681	4.0275	6.442	1.607	-0.533	11.959	-49.0	-53.6	-37.7	...	V
HD 130694	11.4440	4.411	1.392	-0.296	13.477	-61.9	-76.0	+19.4	0.15	

**Table 7** Candidate giant stars of the  $\eta$  Cephei moving group

Star	$\pi$ (mas)	$V$	$(B - V)$	$M_V$	$(FUV - B)$	$U$ (km s $^{-1}$ )	$V$ (km s $^{-1}$ )	$W$ (km s $^{-1}$ )	$E(G_{BP} - G_{RP})$	Notes
HD 4730	10.0981	5.586	1.312	0.607	13.860	-16.2	-66.3	-15.4	0.14	
HD 6254	5.4105	8.014	0.990	1.680	12.933	-32.4	-88.9	-55.8	...	
HD 43380	8.5429	6.390	1.109	1.048	13.694	-17.4	-66.4	-24.4	0.05	
HD 93132	4.5141	6.350	1.565	-0.377	12.674	-39.6	-72.0	-4.7	0.18	
HD 121146	9.9479	6.355	1.105	1.344	14.722	-33.0	-94.1	+2.4	0.16	
HD 125932	19.2042	4.783	1.313	1.200	13.909	-14.2	-59.4	+5.1	0.24	V
HD 217902	8.8748	5.374	1.450	0.115	13.259	-8.8	-65.4	-6.1	0.25	

for three of the stars that Eggen proposed as members (see also Boyle and McClure 1975).

### 3 Data compilation for moving groups

Starting with initial lists of giant stars drawn from the sources referenced above for each of the seven moving groups considered in this paper a search was made for *GALEX* FUV photometry and a variety of ancillary information including Johnson *BV* photometry. The main source from which  $V$  magnitudes and  $B - V$  colours were obtained is the General Catalogue of Photometric Data (GCPD; Mermilliod et al. 1997). A secondary source used for  $B$  and  $V$  magnitudes was the University of Strasbourg's SIMBAD data base (Wenger et al. 2000). Stellar parallax measurements  $\pi$  given by SIMBAD are listed in Tables 1–7. In most cases these are from *Gaia* DR2 measurements (*Gaia* Collaboration 2016, 2018), with *Hipparcos* data (Perryman et al. 1997) constituting much of the rest. Stars for which there was lack of a parallax measurement in SIMBAD were removed from the listings.

Additional information about the nature of some stars was gleaned from SIMBAD, and is recorded in Tables 1–7 using the following abbreviations: unspecified variable star (V), long-period variable (LPV), and Mira variable (MV). Stars which SIMBAD listed as either a RR Lyrae pulsator or post-asymptotic giant branch star have not been included

herein, since these are distinct from the red giant branch in the H-R diagram. Furthermore, stars in our initial lists that were designated in SIMBAD as either a spectroscopic binary or member of a double system have been removed from consideration because of concern that *GALEX* FUV measurements in these cases may be influenced by the presence of FUV light from a companion. This resulted in, for example, the exclusion of  $\sigma$  Pup (HD 59717) itself from the stars listed in Table 6. Similarly, giants were removed from consideration when there was another star within several arc seconds listed in the *Gaia* DR2 data set. Two stars designated by SIMBAD as being in the horizontal branch (HB) phase of evolution are included here because at the metallicities of the Hyades and Wolf 630 groups such stars tend to be located close to the first-ascent red giant branch in the H-R diagram.

Components of space motion for the candidate group stars were calculated by using an applet<sup>1</sup> written by David R. Rodriguez in 2010 (Rodriguez et al. 2011), which in turn is based on the GAL\_UVW program from the IDL Astronomy User's Library.<sup>2</sup> Parallaxes and proper motions from the *Gaia* DR2 were used as inputs. Radial velocities when available from *Gaia* DR2 were also adopted, and for the relatively small fraction of stars for which these were not available, velocities as given by SIMBAD were made use of.

<sup>1</sup><http://www.astro.ucla.edu/~drodrigu/UVWCalc.html>.

<sup>2</sup><https://idlastro.gsfc.nasa.gov/homepage.html>.



**Table 8** Summary of properties of giant star samples for seven moving groups

Group	Age (Gyr)	[Fe/H]	$\sigma(U)$ (km s <sup>-1</sup> )	$\sigma(V)$ (km s <sup>-1</sup> )	$\sigma(W)$ (km s <sup>-1</sup> )
Hyades	0.63	+0.14	7.2	4.1	13.2
Wolf 630	2.7	near-solar	14.4	9.3	19.3
Ursa Major	0.24–0.5	near-solar	4.0	4.4	4.6
HR 1614	2–4	+0.25	13.0	5.4	16.1
$\zeta$ Herculis	3.5	near-solar	16.0	10.7	17.0
$\sigma$ Puppis	...	$\sim -0.4$	19.9	16.6	25.9
$\eta$ Cephei	2.5	$\sim -0.2$	11.7	13.1	21.0

The applet of Rodriguez calculates the  $UVW$  components of space motion, where  $U$  is defined as positive towards the Galactic Center,  $V$  is positive in the direction of Galactic rotation,  $W$  is positive towards the North Galactic Pole, and there is no correction for solar motion. Values of these velocity components in units of km s<sup>-1</sup> are listed for the group candidates in Tables 1–7.

The *GALEX* FUV magnitude encompasses light within a wavelength range of 1350–1750 Å (Martin et al. 2005; Morrissey et al. 2007). The Mikulski Archive for Space Telescopes (MAST) was used to search the *GALEX* Data Release 6/7 for FUV magnitude measurements. Most detections come from images in the *GALEX* All-Sky Survey as opposed to deeper images obtained in response to Guest Investigator programs. Using SIMBAD to obtain the Equatorial sky coordinates, FUV detections were sought within a radius of 0.2 arcmin around each stellar position. The apparent FUV magnitudes employed here remain on the *GALEX* GR6/7 AB system. Although Camarota and Holberg (2014) have investigated corrections to the GR6/7 system, many of the red giants in our moving group survey have apparent FUV magnitudes fainter than the limit of the Camarota and Holberg (2014) recalibration. In the case of stars for which more than one FUV magnitude measurement was listed in the GR6/7 data base the mean value of the multiple FUV measurements was adopted.

The FUV magnitudes were combined with the  $B$  and  $V$  photometry to derive a colour index which is denoted herein as  $(FUV - B)$ . The results are listed in Tables 1–7. Stars from our initial listings which were not found in the GR6/7 data base have been dropped from consideration. Multiple FUV data where available served as a basis for calculating an observational uncertainty in the apparent FUV magnitudes by applying a recipe from small sample statistics as presented in Wan et al. (2014). A representative standard deviation  $\sigma$  in the FUV magnitude data was deduced to be  $\sigma = 0.17$ .<sup>3</sup> The uncertainties in FUV magnitude from *GALEX* dominate the error in the  $(FUV - B)$  colour.

<sup>3</sup>An individual value of  $\sigma$  was calculated from the range between separate FUV magnitude values for each star for which multiple measurements were given by the DR6/7 search. The representative value of  $\sigma$

No attempt was made to correct the observed  $(FUV - B)$  and  $(B - V)$  colours of the group candidates for interstellar reddening. These stars are at a wide range of distances and Galactic coordinates, making precise reddenings difficult to derive. A search was made for values of the interstellar reddening  $E(G_{BP} - G_{RP})$  in the *Gaia* DR2 photometric system and where available these are listed in Tables 1–7. A substantial fraction of group candidates have no such values. The algorithm by which this reddening is derived from the *Gaia* colours of a star is described by Andrae et al. (2018). It is important to note that these reddening values have non-negligible uncertainties to the extent that we have not attempted to use them to correct any of the  $(FUV - B)$  colors in Tables 1–7. Instead these reddening values are used here only for the purpose of identifying stars that may be in sight lines of significant interstellar extinction. As a consequence it is observed colours that are given in Tables 1–7 and plotted in all figures for the moving group candidate giants. Differences in interstellar reddening could thus contribute to scatter in the photometric diagrams contained within this paper.

A summary of the ages and metallicities of the moving groups considered in this paper is given in Table 8, where these data have been obtained from the references noted in the previous section. Standard deviations in the components of space velocity,  $\sigma(U)$ ,  $\sigma(V)$ , and  $\sigma(W)$ , were calculated specifically for the samples of group candidates listed in Tables 1–7, and the results are entered in Table 8 as well.

#### 4 The open cluster NGC 752

Far-ultraviolet photometry is available for a small number of red giants in the open cluster NGC 752. In addition to the All-Sky Survey images, deep *GALEX* images in the vicinity of the cluster were obtained for several Guest Investigator programs (GI1 055001 NGC0752, GI5 063001 A262 FIELD2, and GI5 063001 A262 FIELD3). Associated data

quoted herein is taken to be the mean of these individual values. Some variable stars and flare stars were not considered in this calculation.

**Table 9** Giant stars of NGC 752

WEBDA ID	RA (2000)	Dec (2000)	V	B - V	(FUV - B)	(B - V) <sub>0</sub>	(FUV - B) <sub>0</sub>
001	01:55:12.62	+37:50:14.4	9.496	0.954	12.86	0.914	12.74
075	01:56:18.90	+37:58:00.4	8.971	1.003	13.83	0.963	13.71
077	01:56:21.65	+37:36:08.2	9.375	1.029	13.73	0.989	13.61
110	01:56:50.44	+38:01:58.1	8.961	0.811	8.96	0.771	8.84
137	01:57:03.12	+38:08:02.6	8.927	1.026	14.03	0.986	13.91
208	01:57:37.62	+37:39:37.8	8.958	1.085	13.30	1.045	13.18
213	01:57:38.97	+37:46:12.2	9.041	1.004	13.69	0.964	13.57
295	01:58:29.84	+37:51:37.4	9.303	0.963	13.42	0.923	13.30

for NGC 752 giants are listed in Table 9. The star designations (WEBDA ID) and sky coordinates are from the WEBDA database (Netopil et al. 2012). Only red giants with proper-motion membership probabilities greater than 90% as listed in WEBDA are considered herein. The primary source of the Johnson photometry compiled in Table 10 is Daniel et al. (1994) as obtained from WEBDA.

The age of NGC 752 was found by Agüeros et al. (2018) to be 1.3 Gyr, while the metallicity is very close to that of the Sun (Hobbs and Thorburn 1992, Sestito et al. 2004; Carrera and Pancino 2011). With regard to the interstellar reddening for NGC 752 we adopt the value of  $E(B - V) = 0.04$  from Taylor (2007). Sun et al. (2018) have published a comprehensive study of interstellar extinction in the *GALEX* photometric bandpasses and conclude that  $E(FUV - B) = 3.4E(B - V)$ . By comparison the absorption ratio of  $R(FUV) = 6.8$  from Fitzpatrick (1999) leads to  $E(FUV - B) = 2.7E(B - V)$ . Consequently the reddening to NGC 752 in the FUV is taken to be  $E(FUV - B) = 3.0E(B - V) = 0.12$ . Both the observed  $(FUV - B)$  and  $B - V$  colours as well as the reddening corrected colours  $(FUV - B)_0$  and  $(B - V)_0$  are listed in Table 9.

## 5 Colour-magnitude diagrams

The recent availability of *Gaia* DR2 parallaxes makes it worthwhile to visit the  $(M_V, B - V)$  colour-magnitude diagram (CMD) of the moving group giants. Figure 1 shows the CMD for the Hyades group candidates. Symbols used in this figure are an attempt to provide some indication of the relative likelihood of group membership. The mean value of the  $V$  space motion component for the stars in Table 1 is  $V_m = -17.4 \text{ km s}^{-1}$ . Filled circles denote the most likely stars to be Hyades group giants, which are defined as having velocity components of  $V = (V_m \pm 4.0) \text{ km s}^{-1}$  together with *Gaia* reddenings of  $E(G_{BP} - G_{RP}) < 0.2$  mag. Of more uncertain membership are the candidates shown as open circles, corresponding to stars with velocities  $V < (V_m - 4.0) \text{ km s}^{-1}$  or  $V > (V_m + 4.0) \text{ km s}^{-1}$

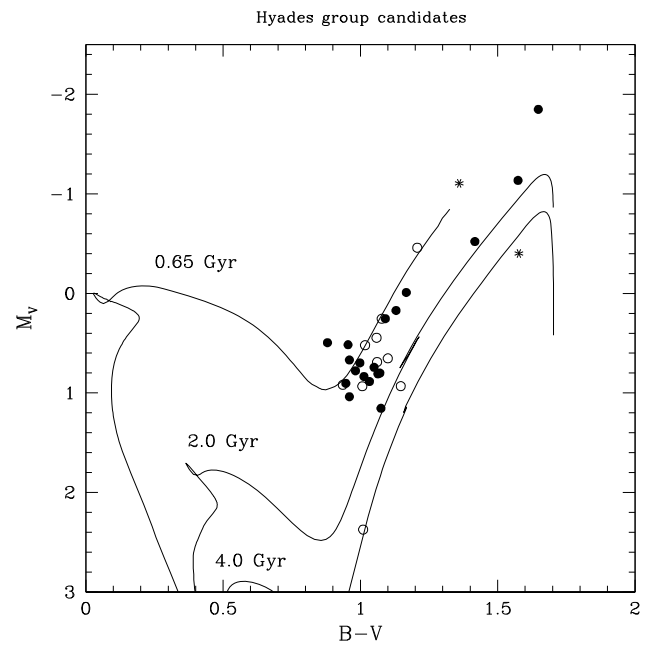


**Fig. 1** Colour-magnitude diagram of the Hyades moving group candidates from Table 1. Dartmouth isochrones for solar abundance and ages of 0.65, 2.0 and 4.0 Gyr are shown as solid lines. Filled circles denote Hyades group candidates with velocity components  $V = -17.4 \pm 4.0 \text{ km s}^{-1}$  and reddenings of  $E(G_{BP} - G_{RP}) < 0.2$  mag. Open circles denote stars that have  $V$  velocities  $> 4 \text{ km s}^{-1}$  removed from the mean of the stars in Table 1 plus reddenings of  $E(G_{BP} - G_{RP}) < 0.2$ . Eight-point asterisks denote stars with  $E(G_{BP} - G_{RP}) \geq 0.2$  regardless of space motion

and reddenings of  $E(G_{BP} - G_{RP}) < 0.2$  mag. Stars with  $E(G_{BP} - G_{RP}) \geq 0.2$  irrespective of space motion are depicted with eight-point asterisks. In order to provide some comparison, Dartmouth isochrones (Dotter et al. 2008) for a solar metallicity and ages of 0.65, 2.0, or 4.0 Gyr are included in Fig. 1 as solid lines. The isochrone for 0.65 Gyr is situated blueward of the majority of data points for the proposed Hyades group giants, but this may be partly a consequence of an above-solar metallicity. There is a preference for many of the Hyades group giants to congregate in a region of the CMD that can be loosely defined by the limits



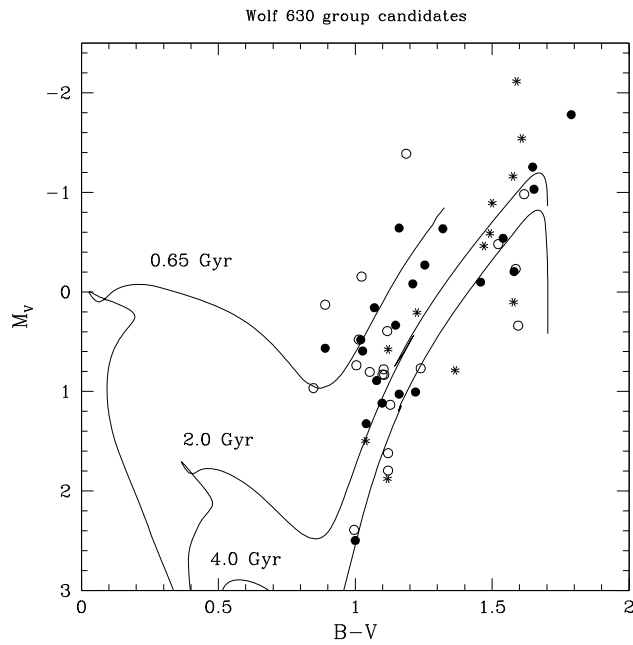


**Fig. 2** Colour-magnitude diagram of the Wolf 630 group candidates from Table 2. Filled circles denote Wolf 630 group candidates with velocity components  $V = -33.8 \pm 5.0 \text{ km s}^{-1}$  and reddenings of  $E(G_{BP} - G_{RP}) < 0.2$ . Open circles denote stars that have  $V$  velocities  $> 5 \text{ km s}^{-1}$  removed from the mean of the stars in Table 2 plus reddenings of  $E(G_{BP} - G_{RP}) < 0.2$ . Eight-point asterisks denote stars with  $E(G_{BP} - G_{RP}) \geq 0.2$  regardless of space motion. Dartmouth RGB isochrones for solar abundance and an age of 0.65, 2.0 and 4.0 Gyr are shown as solid lines

$0.9 < B - V < 1.2$  and  $+0.5 < M_V < +1.0$ . Such stars are potentially in the core-helium-burning (CHB) phase of evolution, whereas giants redward of this region could be either in the first or second ascent of the red giant branch (RGB). Several stars which fall near the 4 Gyr isochrone in Fig. 1 are of uncertain membership status or of high reddening.

Figure 2 shows the CMD of the red giant candidates of the Wolf 630 group from Table 2. The mean component of  $V$  velocity for these stars is  $V_m = -33.8 \text{ km s}^{-1}$ . Filled circles again denote stars that are considered more likely to be group giants, defined in this case as having  $V = (V_m \pm 5.0) \text{ km s}^{-1}$  and  $E(G_{BP} - G_{RP}) < 0.2 \text{ mag}$ . More uncertain candidates for group membership are shown as open circles, corresponding to stars with velocities  $|V - V_m| > 5.0 \text{ km s}^{-1}$  together with  $E(G_{BP} - G_{RP}) < 0.2$ . All Wolf 630 group candidates with  $E(G_{BP} - G_{RP}) \geq 0.2$  are plotted as eight-point asterisks. Solar-abundance Dartmouth isochrones for ages 0.65, 2.0 and 4.0 Gyr are again plotted in Fig. 2. The Wolf 630 giant candidates exhibit a greater scatter within the red giant region of the CMD than do the Hyades candidates, and even those stars with close-to-average space motion are dispersed between the 0.65 and 4.0 Gyr isochrones. On average, the Wolf 630 candidates are displaced redward of the Hyades group RGB, consistent with a greater age for the Wolf 630 group. However, there

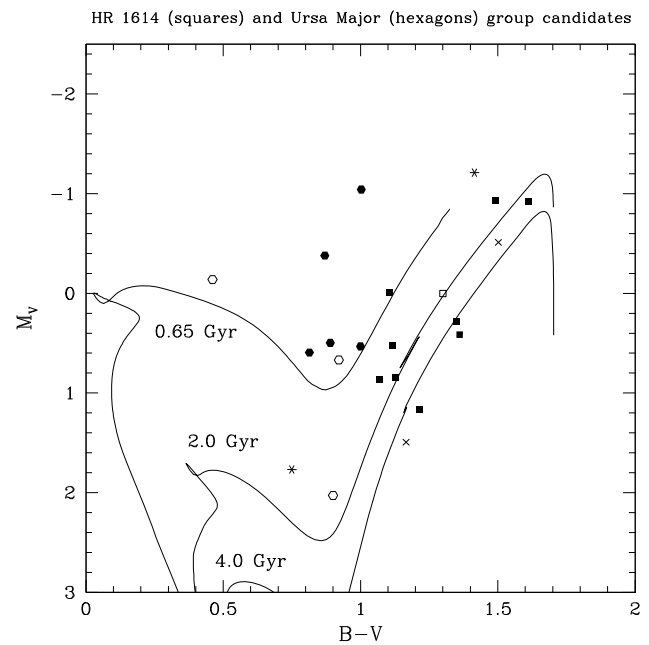


**Fig. 3** Colour-magnitude diagram of the candidate giants for the Ursa Major moving group (filled and open hexagons or six-pointed asterisks) compared with candidates for the HR 1614 group (filled and open squares or four-pointed crosses). Filled symbols depict stars considered more likely to be group members according to the kinematic criteria noted in the text. Dartmouth solar-abundance isochrones for first-ascendant red giants of age 0.65, 2.0 or 4.0 Gyr are shown as solid lines

are some Wolf 630 candidates that fall close to the Hyades giant branch, while others fall in the vicinity of the 4 Gyr isochrone. This implies that there may be a considerable admixture of non-group members included in Table 2 and Fig. 2.

Figure 3 presents the CMD of the candidate giants for the Ursa Major and HR 1614 groups from Tables 3 and 4, along with 0.65, 2.0 and 4.0 Gyr Dartmouth isochrones. The standard deviations in all three velocity components for the Ursa Major candidates are relatively small; in the case of group candidates with  $E(G_{BP} - G_{RP}) < 0.2$  the closed hexagons in Fig. 3 depict stars with  $U = (U_m \pm 4.0) \text{ km s}^{-1}$ , while open hexagons denote giants outside this range of velocities. The mean value of the  $U$  component for the sample from Table 3 is  $U_m = 15.2 \text{ km s}^{-1}$ . Filled and open squares are used in analogous fashion in Fig. 3 to depict candidates of the HR 1614 group, with the filled symbols corresponding to stars having a kinematic criterion of  $V = (V_m \pm 6.0) \text{ km s}^{-1}$ , where  $V_m = -56.4 \text{ km s}^{-1}$  among the stars of Table 4. Ursa Major and HR 1614 group candidates with  $E(G_{BP} - G_{RP}) \geq 0.2$  are shown by six-pointed asterisks and four-pointed crosses respectively.

Candidate giants of the Ursa Major group fall on average to the blue of the 0.65 Gyr isochrone, consistent with this group being of a younger age than the Hyades group. Nevertheless, the Ursa Major group candidates do not obvi-

ously define a single-age sequence in the colour-magnitude diagram. Giants proposed for the HR 1614 group mostly fall redward of the Hyades group RGB, consistent with the former being of an older age and slightly higher metal abundance. Many of the HR 1614 giant candidates locate near the 2–4 Gyr isochrones, while several fall close to the CHB region of the colour-magnitude diagram. For example, should HD 40176 prove to be a member of the HR 1614 group it may be in the asymptotic giant branch (AGB) phase of evolution, having only recently evolved away from the CHB stage. The candidate giants of the HR 1614 group exhibit one of the better-defined CMDs of the samples considered here, which seems to accord with the finding of De Silva et al. (2007) that a kernel of chemically homogeneous stars can indeed be identified among those selected to have kinematics similar to the eponymous star.

The notable dispersion of the Wolf 630 and Ursa Major giants within the CMD that is seen when using *Gaia* parallaxes may indicate that not all of the giants in Tables 2 and 3 are members of these groups, and that not all group candidates are of the same age. Hence the use of the term “quasi-coeval” in the title of this paper to describe the samples of giants that have been compiled here. It is not an objective here to attempt a statistical assessment of group likelihood for the stars in Tables 1–7, but it is emphasised that the Hyades, Wolf 630, Ursa Major and HR 1614 samples selected here may contain a substantial fraction of group non-members.

The candidate giants for the proposed  $\zeta$  Herculis,  $\eta$  Cephei, and  $\sigma$  Puppis groups are collectively plotted in the colour-magnitude diagram of Fig. 4. Data points for all three groups are mainly located redward of the 2 Gyr isochrone, and all fall redward of the Hyades group candidates from Table 1 which are shown for comparison in Fig. 4 as filled circles. Substantial dispersions are found in all three space motion components among the  $\zeta$  Herculis,  $\eta$  Cephei, and  $\sigma$  Puppis samples (Table 8). The exact number of red giants within these groups would seem to require further analysis.

## 6 Two-colour diagrams

A two-colour diagram showing  $(FUV - B)$  versus  $B - V$  for stars of the Hyades moving group is presented in Fig. 5, in which circles and asterisks depict the giants from Table 1, while open squares show dwarf stars of this group from the data of Cochrane and Smith (2019). The symbols for the giants in Fig. 5 follow the same convention as for Fig. 1, so that filled circles correspond to giants with a smaller range in the  $V$  velocity than the open circles. The locus of field dwarf stars in such a two-colour diagram was discussed by Smith and Redenbaugh (2010). By and large the RGB stars of the Hyades group evince a separate locus from the main sequence stars in this FUV two-colour space. The

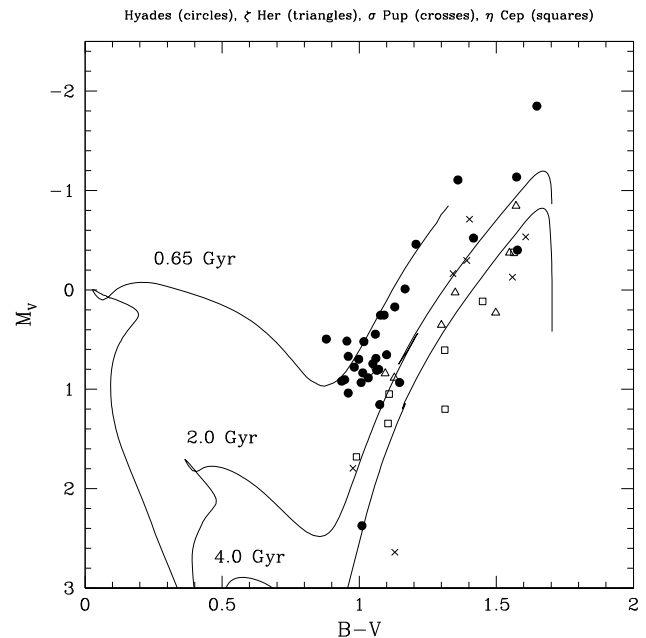


**Fig. 4** Collective colour-magnitude diagram for candidate giants of the moving groups proposed to be associated with  $\zeta$  Herculis (open triangles),  $\sigma$  Puppis (crosses), and  $\eta$  Cephei (open squares) from Tables 5–7. Filled circles define Hyades group candidates from Table 1. Dartmouth RGB isochrones for solar abundance and ages of 0.65, 2.0 or 4.0 Gyr are shown as solid lines

majority of the core-He-burning stars fall among those giants with the very reddest  $(FUV - B)$  colours in a region near  $(FUV - B, B - V) \sim (14.0 \pm 0.5, 1.0 \pm 0.1)$ . By comparison, the dwarf stars with the reddest FUV colours have  $(FUV - B) \sim 12.0$ . In the colour range  $0.85 < (B - V) < 1.05$  there are a few Hyades group giants, notably in the CHB phase, that encroach into the domain defined by the dwarf stars. A range in FUV luminosity at a given effective temperature among Hyades group CHB giants would imply also a range in Mg II  $h$  and  $k$  emission line strengths if the correlations documented among field giants by Smith (2018, 2019) apply. If so, this would parallel findings by Baliunas et al. (1983) and Schröder et al. (2020) of a range in strength of the Mg II  $hk$  lines and other chromospheric and coronal indicators such as  $\lambda 1548$  C IV among giants of the Hyades open cluster. Such exceptions aside, most of the Hyades group dwarf and giant stars are offset from each other in the two-colour diagram and define separate sequences. Among Hyades group giants with  $(B - V) > 1.2$  the ratio of the FUV-band flux to  $B$ -band flux increases towards cooler effective temperatures, as is also the case along the dwarf sequence.

The Ursa Major moving group and the open cluster NGC 752 straddle the Hyades group in age, with the former being about twice as young as the Hyades and the later about twice as old. Two-colour diagrams of these three systems are compared in Fig. 6, with Ursa Major group giants be-

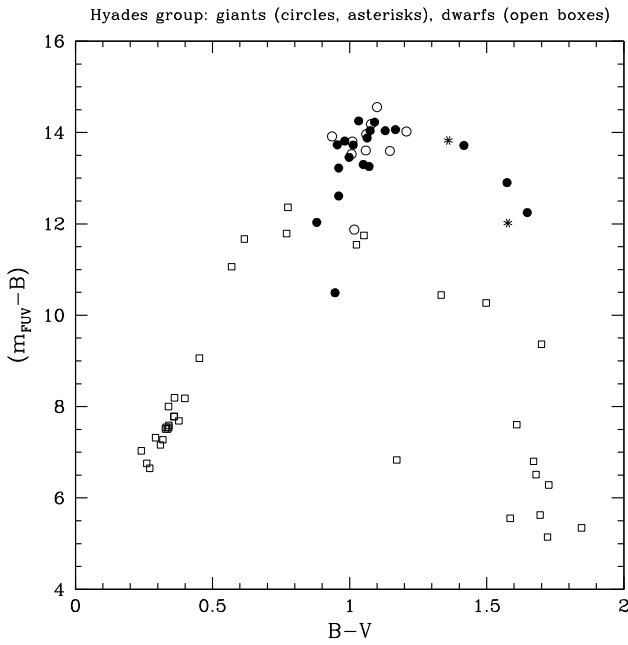


**Fig. 5** A two-colour diagram showing  $(FUV - B)$  versus  $B - V$  for giant stars (from Table 1) that are candidates for membership of the Hyades group. The symbol convention used here is the same as in Fig. 1. Filled circles again denote candidate giants with  $V = -17.4 \pm 4.0 \text{ km s}^{-1}$  and a reddening of  $E(G_{BP} - G_{RP}) < 0.2$  mag. Open circles correspond to giants outside this range of  $V$  velocity in addition to having  $E(G_{BP} - G_{RP}) < 0.2$ . Eight-point asterisks designate giants with  $E(G_{BP} - G_{RP}) \geq 0.2$  irrespective of space motion. Shown for comparison are dwarf stars of the Hyades group (open squares), the data for which come from Cochrane and Smith (2019)

ing shown as open circles and the NGC 752 cluster giants as filled circles. The data points for NGC 752 have been corrected for the interstellar reddenings described in Sect. 4. Giants from NGC 752 occupy the CHB region of Fig. 6 and overlap closely with the Hyades group giants (which are shown as filled triangles). This is also the case for the small sample of Ursa Major candidates, whose giants blueward of  $B - V \sim 1.1$  mag show a tendency to duplicate the broad range in  $(FUV - B)$  that is found among such Hyades group giants. By contrast, although all of the NGC 752 giants in Fig. 6 have an optical colour of  $B - V \sim 1.1$ , they do not evince as large a range in  $(FUV - B)$  as Hyades or Ursa Major candidates.

The Wolf 630 group offers a system that is some four times as old as the Hyades group, with a total difference of about 2 Gyr in age. The two-colour diagram of the candidate giants for the Wolf 630 group is shown in Fig. 7. The symbols are described in the figure caption and are the same as for Fig. 2, i.e., the filled circles potentially represent those stars with the highest likelihood of group membership. With the exception of four Wolf 630 group stars at  $(FUV - B) \sim 13.0 \pm 0.5$  and  $B - V \sim 1.15 \pm 0.05$  the giants of the Hyades and Wolf 630 groups trace much the same locus in the FUV two-colour diagram. Quite a few of

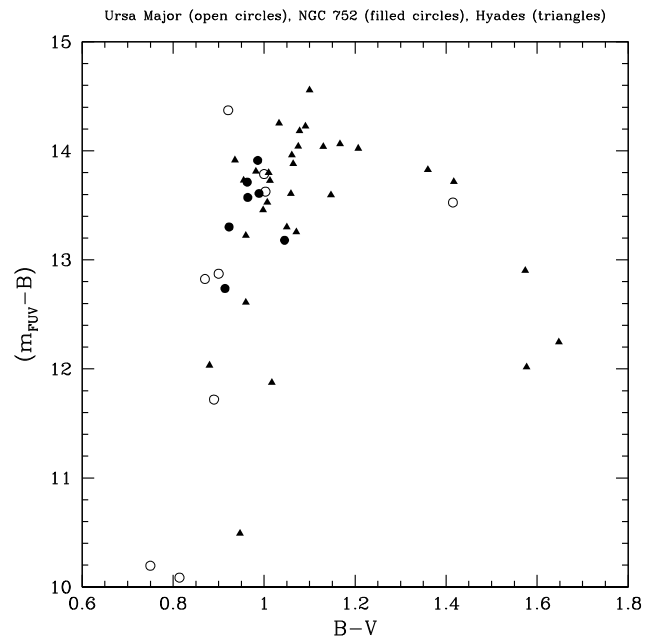


**Fig. 6** The  $(FUV - B)$  versus  $B - V$  two-colour diagram for red giants of the Ursa Major (open circles) and Hyades (filled triangles) moving groups together with giants of the open cluster NGC 752 (filled circles). The colours plotted for NGC 752 are the reddening-corrected values from Table 9

the Wolf 630 giants fall in a similar region of the two-colour diagram to the Hyades core-helium-burning stars. By and large, the giants in the two groups are indistinguishable in the two-colour diagram, with the exception of four Wolf 630 giants near  $B - V \sim 1.2$  which are about 1 magnitude bluer in  $(FUV - B)$  than both the Hyades giants and other Wolf 630 stars of comparable optical colour. If one or more of these four stars are physical members of the Wolf 630 system then they reveal a scatter in stellar activity among the CHB stars of this group, possibly analogous to that evinced among the somewhat bluer Hyades CHB candidates (Fig. 5).

At least as old as the Wolf 630 group, if not older, the HR 1614 group comprises red giants that are potentially higher in metallicity than those of the Hyades group. The giant stars from these two systems are compared in Fig. 8. All but one of the HR 1614 group giants fall near a locus for  $B - V > 1.0$  that closely follows the region of the Hyades giants. There is one giant nonetheless, HD 40176, that exhibits a pronounced FUV excess of some 2 mag. This star may be a further example of a range of stellar activity in the CHB region of the two-colour diagram.

The  $\zeta$  Herculis,  $\eta$  Cephei, and  $\sigma$  Puppis giants are shown in the two-colour diagram of Fig. 9. Only modest numbers of giants have been ascribed to these three systems, which may be comparable in age to the Wolf 630 or HR 1614 groups, but again there is little to separate them in the two-colour diagram from the giants of the Hyades group (which are shown for comparison). There are no obvious FUV-excess

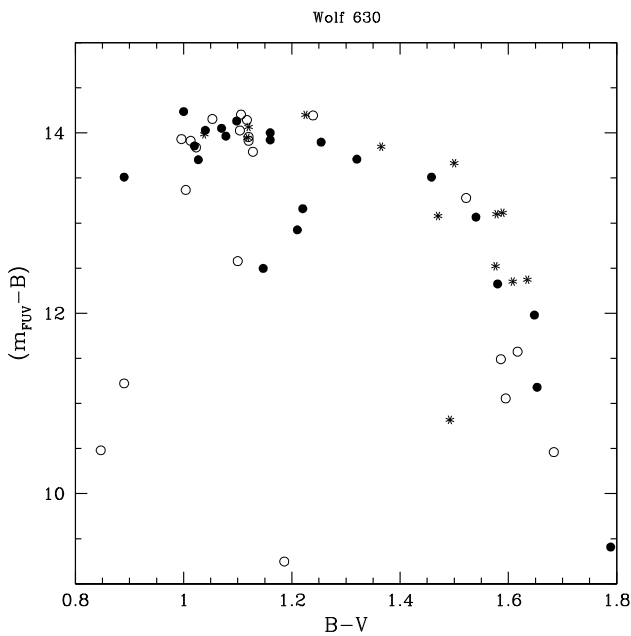


**Fig. 7** Red giant candidates of the Wolf 630 moving group (from Table 2) in the  $(FUV - B)$  versus  $B - V$  two-colour diagram. In accord with Fig. 2, filled circles again denote candidate giants with  $V = -33.8 \pm 5.0 \text{ km s}^{-1}$  and  $E(G_{BP} - G_{RP}) < 0.2 \text{ mag}$ , open circles correspond to giants outside this range of  $V$  velocity for which  $E(G_{BP} - G_{RP}) < 0.2$ , and eight-point asterisks denote all giants with  $E(G_{BP} - G_{RP}) \geq 0.2$

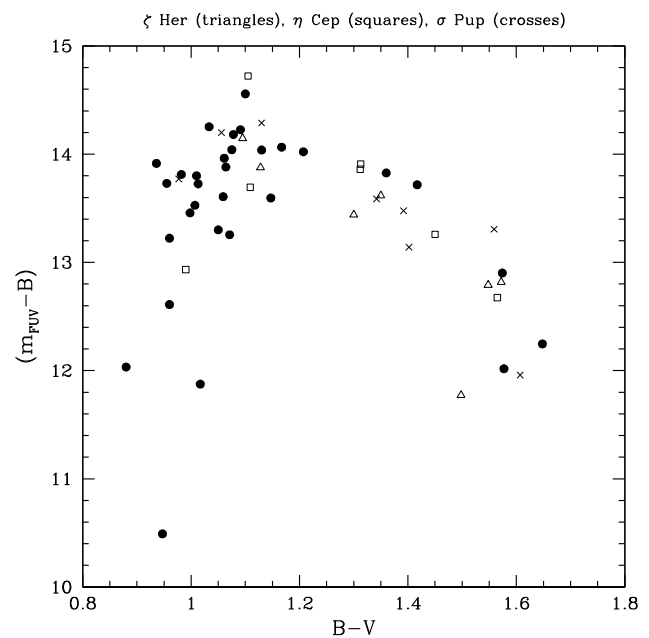


**Fig. 9**  $(FUV - B)$  versus  $B - V$  two-colour diagram for red giants of the  $\zeta$  Herculis (triangles),  $\eta$  Cephei (squares),  $\sigma$  Puppis (crosses) and Hyades (filled circles) moving groups

CHB giants in these three groups, although the sample sizes are relatively small, and membership of individual stars is not well constrained by the space motion data.

## 7 Conclusions

A summary of the patterns seen among the candidate giants of the seven moving groups considered in this paper can be found in Figs. 10 and 11. Giants from Tables 1 through 7 inclusive are collectively plotted in the colour-magnitude diagram of Fig. 10 wherein different symbols are used to designate the phase of stellar evolution: open circles denote stars whose CMD position is consistent with a core-helium-burning stage of evolution, crosses denote giants fainter than  $M_V \sim +1.0$  which are most likely in their first ascent of the lower-RGB, while filled circles denote higher luminosity stars that could be either in the first or second ascent of the giant branch. Several solar-abundance Dartmouth isochrones are plotted for comparison, thereby illustrating the range in age among the groups chosen for this study.

On top of a spread in age between groups, none of the samples collected in Tables 1–7 define as tight a sequence in the CMD as is customary among open clusters. Furthermore, there is notable dispersion in space velocity, particularly in the  $U$  and  $W$  components, among the giants within each set of group candidates, as indicated by the standard deviations listed in Table 8. Thus the samples assembled for

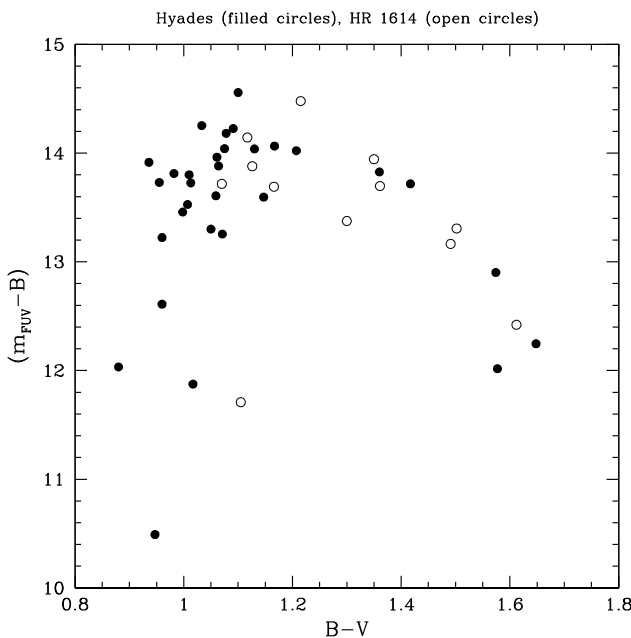


**Fig. 8** Red giants of the HR 1614 moving group (open circles) in the  $(FUV - B)$  versus  $B - V$  two-colour diagram. Hyades group giants are included as filled circles

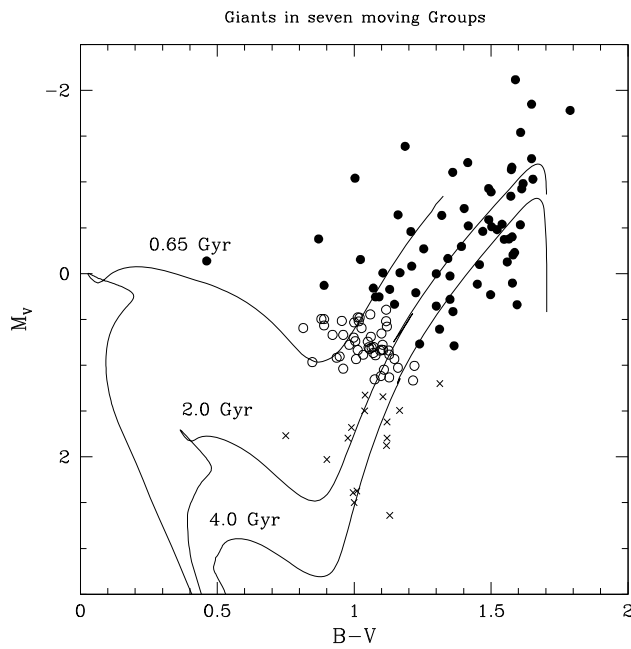


**Fig. 10** Collective colour-magnitude diagram for the candidate giants of seven moving-groups as appearing in Tables 1–7. Crosses show lower-RGB stars making a first ascent of the giant branch, while filled circles correspond to upper-RGB stars in either the first or second ascent of the giant branch. Open circles depict stars that may be in a core-He-burning phase of evolution. Dartmouth RGB isochrones for solar abundance and an age of 0.65, 2.0 and 4.0 Gyr are shown as solid lines

Tables 1–7 are likely to be inhomogeneous with regard to group membership, and the number of true red giants in the  $\zeta$  Herculis,  $\eta$  Cephei,  $\sigma$  Puppis groups may be particularly small. Hence of the kinematic samples considered here only the giants in the open cluster NGC 752 should be considered as truly coeval.

Figure 11 shows a collective ( $FUV - B, B - V$ ) two-colour diagram for all seven groups with the symbols again being encoded to distinguish lower-RGB, CHB, and upper-RGB stars. In general, the giant star candidates of the moving groups studied here fall largely in overlapping regions of the  $FUV$  two-colour diagram, with little apparent offset between groups of different age. The giant-star two-colour sequence displays a maximum near  $(FUV - B) \approx 14.2$  within the colour range  $1.0 < B - V < 1.25$ . On the red side of this maximum the group RGB stars tend to follow a common locus at  $B - V > 1.25$ . Unlike the dwarf sequences of moving groups, which exhibit offset loci in the ( $FUV - B, B - V$ ) two-colour diagram that correlate with group age, even at  $B - V$  colours redward of 1.20 mag (Cochrane and Smith 2019), the reddest giants studied here all follow similar two-colour loci regardless of group identity. Among giants with  $0.8 \leq B - V \leq 1.2$  there is a substantial scatter in ( $FUV - B$ ) of 2–4 mag at a given  $B - V$  which can be discerned within the CHB and upper-RGB locations of the

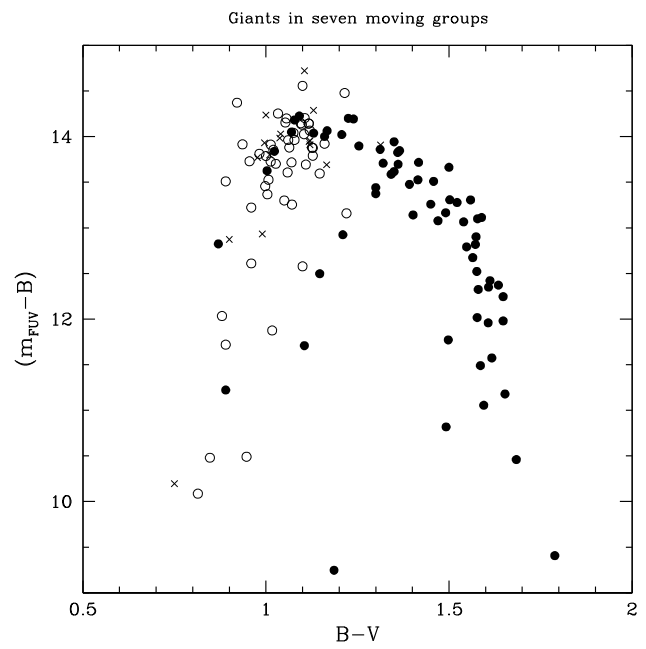


**Fig. 11** Collective ( $FUV - B, B - V$ ) two-colour diagram for moving-group stars from Tables 1–7. Open circles depict core-He-burning stars as identified in Fig. 10, crosses show lower-RGB stars making a first ascent of the giant branch, while filled circles correspond to upper-RGB stars in either the first or second ascent of the giant branch

CMD, but may be more marked for the CHB stars. This may be suggestive of a range in chromospheric activity, such as that seen among field giants by Smith (2018), and observed among the giants of the Hyades open cluster (Baliunas et al. 1983).

### 7.1 Trends with effective temperature

The giants in this paper encompass a broad range of effective temperature. The behaviour of ( $FUV - B$ ) colour as a function of effective temperature will depend upon factors that include (i) how the photospheric flux in both the  $FUV$  and  $B$  bands varies with effective temperature, and (ii) how the emission line spectrum from the chromosphere and transition region varies with effective temperature. In a case where photospheric light dominates the flux in the  $FUV$  band the ( $FUV - B$ ) colour would be expected to become redder as the  $B - V$  colour becomes redder. This is seen in Fig. 5 among the Hyades main sequence stars with  $(B - V) < 0.8$ , but the giant stars in the moving groups studied here do not populate this colour space. The *IUE* SWP spectra of Ayres et al. (1981) reveal a marked contrast between G and K giants in the photospheric contribution to the  $FUV$  spectrum.

One photospheric factor that will be pertinent as a function of effective temperature among late-type stars is the increasing bolometric correction of the photospheric  $B$ -band light upon moving to a cooler temperature. If the ratio of  $FUV$ -to-bolometric luminosity were to remain constant for



all giants redder than  $B - V = 1.0$ , the  $(FUV - B)$  colour would become bluer as the  $B - V$  colour becomes redder due to this bolometric correction effect. This may most notably influence the behaviour of  $(FUV - B)$  in the cooler half of the two-colour diagram, both in the case of giant and dwarf stars (Smith and Redenbaugh 2010). Among the moving group giants the blueward upturn of  $(FUV - B)$  for  $(B - V) > 1.2$  may indicate that the chromospheric and transition region emission-line fluxes are varying less with effective temperature than is the  $B$ -band photospheric flux.

As regards giant stars the excitation states of species in the chromosphere and transition region that produce FUV emission lines is a function of effective temperature. Early spectroscopic studies using *IUE* revealed differences between the emission lines present in the FUV spectra of warm yellow giants as compared to cooler red giants. Ayres et al. (1981) found that a number of FUV emission lines are stronger among G giants than K giants (see Fig. 3 of their paper). In samples of stars studied by Linsky and Haisch (1979) and Simon et al. (1982), the yellow giants exhibited emission lines formed at temperatures as high as  $10^5$  K within a transition region, whereas cooler red giants typically showed lower-temperature lines from a chromosphere. In a spectrum of  $\beta$  Cet (G9.5 III) Eriksson et al. (1983) identified FUV emission lines of high-excitation species such as Si IV and C IV, along with C I and C II lines. Among the K0 III giants of the Hyades cluster the FUV bandpass was found to contain emission lines that include  $\lambda 1335$  C II,  $\lambda 1548$  C IV, and  $\lambda 1657$  C I (Baliunas et al. 1983). However, the strength of some of these lines vary markedly among the Hyades giants despite their similarity of spectral type, with the C IV line ranging by a factor of 6 in emission strength. The spectrum of the K2 giant Arcturus was found by Ayres et al. (1981, 1986) to lack high-excitation transition region lines such as  $\lambda 1548$  C IV, but it does include a number of emission lines from lower-excitation species including some features produced by fluorescence. At the later spectral type of K5 III for  $\alpha$  Tau, McMurray et al. (1999) found a fluorescence spectrum. Linsky (2017) has reviewed the variety of features characteristic of the FUV spectra of both dwarf and giant stars. The above examples for giant stars suggest that the sensitivity of the  $(FUV - B)$  colour to stellar activity might lead to both systematic changes with spectral type and scatter at a given spectral type.

Dupree et al. (1999) found that on the red giant branch of the open cluster M67 there is a well-defined relationship between the level of chromospheric activity and effective temperature. Pasquini and Brocato (1992) attempted to parameterise the chromospheric emission in the Ca II K line against both age and effective temperature by comparing Population II giants with red giants in the Hyades and M67 open clusters, i.e., they compared red giants of age greater than 0.6 Gyr. They found that while there is a very strong correlation

between K-line emission flux and effective temperature, any correlation with age was much weaker and at the level of statistical significance. Within the context of the redder half of the FUV two-colour diagram of red giants, the results of Pasquini and Brocato (1992) seem in accord with the near-identical RGB loci at  $(B - V) > 1.2$  found among the moving groups studied here.

What about the great range in FUV activity seen within the warmer half of the RGB two-colour diagram? When comparing giants of the same  $B - V$  colour drawn from moving groups of different age, a comparison is being made between giants of different mass (as seen from the isochrones in Fig. 1). Thus it might be proposed that the spread detected in  $(FUV - B)$  at a given  $B - V$  among RGB stars with  $(B - V) < 1.2$  may in some part reflect differences in activity that have carried over from different-mass main-sequence progenitor stars. However, the results of Pasquini and Brocato (1992) seem to suggest that any such pre-RGB phenomenon is of second-order compared to processes within the red giants themselves which maintain surface activity. As has been noted above, clues to the origin of the scatter in  $(FUV - B)$  colour at a given effective temperature among giants with  $(B - V) < 1.2$  may come from the range in chromospheric activity observed among the giants of the Hyades open cluster (Baliunas et al. 1983).

## 7.2 Chromospheric changes accompanying red giant branch evolution

Low-mass stars spend much less time in the red giant phase of evolution than in the main sequence phase. Rotational braking plus solar-wind-like mass loss produces a progressive decrease in stellar rotation rate and magnetic activity throughout the main sequence phase of evolution. This mechanism has a timescale of 1-10 Gyr over which it can alter the rotation of a star of mass less than  $2M_{\odot}$ . However, such a mechanism if it continues will have less time to alter the rotation of a star while it is in the red giant phase. Instead the evolution in the rotation of a red giant will be controlled by the redistribution in mass and angular momentum that occurs within the star as it ascends the red giant branch, as the central He-core contracts accompanied by large-scale expansion of the H-rich envelope and the deepening of the convective region within this envelope. During this phase of evolution major changes in interior structure and rotation can occur within a low-mass star on timescales of tens to hundreds of millions of years. Such structural and rotational changes within a red giant could in turn play a major role in controlling the evolution of chromospheric heating, whether this heating process still involves a rotationally-induced solar-type dynamo (Rutten and Pylyser 1988) or not (e.g., Cuntz 1990; Cuntz et al. 1994).

As low-mass stars evolve from the main sequence into the subgiant region of the H-R diagram there is evidence that the



flux in chromospheric and transition region emission lines decreases relative to the bolometric flux (Simon and Drake 1989). Low-mass stars may thereby enter the red giant phase of evolution with reduced diversity in their level of stellar activity. Stellar evolution then modifies this level of activity as stars evolve structurally during the red giant phase.

Strassmeier et al. (1994) found that correlations exist between rotation *speed* and flux in the Ca II K emission line for giant stars hotter than 4500 K (spectral types earlier than  $\sim$  K2). The coolest giants in their survey have a spectral type of K5, and among the small number of K2–K5 giants ( $T_{\text{eff}} = 4500\text{--}4000$  K;  $B - V = 1.1\text{--}1.4$  mag; Bessell 1979) in their survey they did formally find a correlation between K-line emission flux and rotation speed although it is very steep. Analogously, Rutten (1987) had previously found a colour-dependent relationship between Ca II emission and rotation *period* among a mixed sample of dwarf and giant stars extending to a colour as red as  $B - V \sim 1.4$ . Thus rotation seems to be linked to chromospheric activity on the red giant branch (e.g., Gondoin 2018).

Rotation may remain a governing factor for the ( $FUV - B$ ) colour of a low-mass red giant at least until physical processes such as pulsation and mass-loss influence the structure of the chromosphere. In this context, Baliunas et al. (1983) proposed that a range in chromospheric emission discovered among the Hyades cluster giants may be connected to magnetic activity cycles during the core-helium-burning phase of evolution. Schröder et al. (2020) inferred that the Hyades giants have spent different amounts of time in the CHB phase, and suggested that they may be in different stages of internal spindown. Perhaps the range in ( $FUV - B$ ) colour among potential CHB stars in the moving groups considered here may also be associated with differing degrees of internal spin-down during the core-helium-burning phase of evolution.

**Acknowledgements** GHS gratefully acknowledges the support of the National Science Foundation through award AST-1517791.

This research has made use of the NASA Astrophysics Data System. Some of the data presented in this paper were obtained from the Mikulski Archive for Space Telescopes (MAST). STScI is operated by the Association of Universities for Research in Astronomy, Inc., under NASA contract NAS5-26555. This work has made use of data from the European Space Agency (ESA) mission *Gaia*,<sup>4</sup> as processed by the *Gaia* Data Processing and Analysis Consortium (DPAC<sup>5</sup>). Funding for the DPAC has been provided by national institutions, in particular the institutions participating in the *Gaia* Multilateral Agreement.

This research also made use of the SIMBAD data base, operated at CDS, Strasbourg, France, as well as the General Catalogue of Photometric Data operated at the University of Lausanne, Switzerland, and the WEBDA database, operated at the Department of Theoretical Physics and Astrophysics of the Masaryk University.

We thank the referee for helpful comments on the manuscript.

<sup>4</sup><https://www.cosmos.esa.int/gaia>.

<sup>5</sup><https://www.cosmos.esa.int/web/gaia/dpac/consortium>.

**Publisher's Note** Springer Nature remains neutral with regard to jurisdictional claims in published maps and institutional affiliations.

## References

- Affer, L., Micela, G., Morel, T., Sanz-Forcada, J., Favata, F.: *Astron. Astrophys.* **433**, 647 (2005)
- Agüeros, M.A., et al.: *Astrophys. J.* **862**, 33 (2018)
- Andrae, R., et al.: *Astron. Astrophys.* **616**, A8 (2018)
- Asiain, R., Figueras, F., Torra, J.: *Astron. Astrophys.* **350**, 434 (1999)
- Ayres, T.R.: *Astron. J.* **149**, 58 (2015)
- Ayres, T.R., Judge, P., Jordan, C., Brown, A., Linsky, J.L.: *Astrophys. J.* **311**, 947 (1986)
- Ayres, T.R., Marstad, N.C., Linsky, J.L.: *Astrophys. J.* **247**, 545 (1981)
- Baliunas, S.L., Hartmann, L., Dupree, A.K.: *Astrophys. J.* **271**, 672 (1983)
- Barnes, S.A.: *Astrophys. J.* **669**, 1167 (2007)
- Bessell, M.S.: *Publ. Astron. Soc. Pac.* **91**, 589 (1979)
- Bianchi, L.: *Astrophys. Space Sci.* **354**, 103 (2014)
- Bond, H.E., Schaefer, G.H., Gilliland, R.L., et al.: *Astrophys. J.* **840**, 70 (2017)
- Boyle, R.J., McClure, R.D.: *Publ. Astron. Soc. Pac.* **87**, 17 (1975)
- Bubar, E.J., King, J.R.: *Astron. J.* **140**, 293 (2010)
- Camarota, L., Holberg, J.B.: *Mon. Not. R. Astron. Soc.* **438**, 3111 (2014)
- Carrera, R., Pancino, E.: *Astron. Astrophys.* **535**, 30 (2011)
- Cochrane, K.M., Smith, G.H.: *Publ. Astron. Soc. Pac.* **131**, 114201 (2019)
- Cuntz, M.: *Astrophys. J.* **349**, 141 (1990)
- Cuntz, M., Rammacher, W., Ulmschneider, P.: *Astrophys. J.* **432**, 690 (1994)
- Daniel, S.A., Latham, D.W., Mathieu, R.D.: *Publ. Astron. Soc. Pac.* **106**, 281 (1994)
- De Silva, G.M., Freeman, K.C., Bland-Hawthorn, J., Asplund, M., Bessell, M.S.: *Astron. J.* **133**, 694 (2007)
- De Silva, G.M., Freeman, K.C., Bland-Hawthorn, J., Asplund, M., Williams, M., Holmberg, J.: *Mon. Not. R. Astron. Soc.* **415**, 563 (2011)
- Dopcke, G., Porto de Mello, G.F., Sneden, C.: *Mon. Not. R. Astron. Soc.* **485**, 4375 (2019)
- Dotter, A., Chaboyer, B., Jevremović, D., et al.: *Astrophys. J. Suppl. Ser.* **178**, 89 (2008)
- Dupree, A.K., Hartmann, L., Smith, G.H.: *Astrophys. J.* **353**, 623 (1990)
- Dupree, A.K., Lobel, A., Young, P.R., et al.: *Astrophys. J.* **622**, 629 (2005)
- Dupree, A.K., Whitney, B.A., Pasquini, L.: *Astrophys. J.* **520**, 751 (1999)
- Eggen, O.J.: *Mon. Not. R. Astron. Soc.* **118**, 154 (1958)
- Eggen, O.J.: In: Blaauw, A., Schmidt, M. (eds.) *Galactic Structure*, p. 111. University of Chicago Press, Chicago (1965a)
- Eggen, O.J.: *Observatory* **85**, 191 (1965b)
- Eggen, O.J.: *Publ. Astron. Soc. Pac.* **83**, 251 (1971)
- Eggen, O.J.: *Astrophys. J.* **222**, 203 (1978)
- Eggen, O.J.: *Astron. J.* **90**, 74 (1985a)
- Eggen, O.J.: *Astron. J.* **90**, 333 (1985b)
- Eggen, O.J.: *Astron. J.* **90**, 1046 (1985c)
- Eggen, O.J.: *Astron. J.* **112**, 1595 (1996)
- Eggen, O.J.: *Astron. J.* **115**, 2453 (1998)
- Eriksson, K., Linsky, J.L., Simon, T.: *Astrophys. J.* **272**, 665 (1983)
- Famaey, B., Siebert, A., Jorissen, A.: *Astron. Astrophys.* **483**, 453 (2008)
- Feltzing, S., Holmberg, J.: *Astron. Astrophys.* **357**, 153 (2000)
- Findeisen, K., Hillenbrand, L., Soderblom, D.: *Astron. J.* **142**, 23 (2011)

- Fitzpatrick, E.L.: *Publ. Astron. Soc. Pac.* **111**, 63 (1999)
- Gaia Collaboration: *Astron. Astrophys.* **595**, A1 (2016)
- Gaia Collaboration: *Astron. Astrophys.* **616**, A1 (2018)
- Gondoin, P.: *Astron. Astrophys.* **616**, A154 (2018)
- Hobbs, L.M., Thorburn, J.A.: *Astron. J.* **104**, 669 (1992)
- Judge, P.G., Stencel, R.E.: *Astrophys. J.* **371**, 357 (1991)
- King, J.R., Villareal, A.R., Soderblom, D.R., Gulliver, A.F., Adelman, S.J.: *Astron. J.* **125**, 1980 (2003)
- Linsky, J.L.: *Annu. Rev. Astron. Astrophys.* **55**, 159 (2017)
- Linsky, J.L., Haisch, B.M.: *Astrophys. J. Lett.* **229**, L27 (1979)
- Liu, F., Chen, Y.Q., Zhao, G., et al.: *Mon. Not. R. Astron. Soc.* **422**, 2969 (2012)
- Martin, D.C., Fanson, J., Schiminovich, D., et al.: *Astrophys. J.* **619**, L1 (2005)
- McDonald, A.R.K., Hearnshaw, J.B.: *Mon. Not. R. Astron. Soc.* **204**, 841 (1983)
- McMurray, A.D., Jordan, C., Carpenter, K.G.: *Mon. Not. R. Astron. Soc.* **302**, 48 (1999)
- Mermilliod, J.-C., Mermilliod, M., Hauck, B.: *Astron. Astrophys. Suppl. Ser.* **124**, 349 (1997)
- Morel, P., Berthomieu, G., Provost, J., Thévenin, F.: *Astron. Astrophys.* **379**, 245 (2001)
- Morrissey, P., Conrow, Y., Barlow, T.A., et al.: *Astrophys. J. Suppl. Ser.* **173**, 682 (2007)
- Murgas, F., Jenkins, J.S., Rojo, P., Jones, H.R.A., Pinfield, D.J.: *Astron. Astrophys.* **552**, 27 (2013)
- Netopil, M., Paunzen, E., Stütz, C.: In: Moitinho, A., Alves, J. (eds.) *Star Clusters in the Era of Large Surveys*. *Astrophys. Space Sci. Proceedings*, p. 53. Springer, Berlin, Heidelberg (2012)
- Pasquini, L., Brocato, E.: *Astron. Astrophys.* **266**, 340 (1992)
- Pasquini, L., Brocato, E., Pallavicini, R.: *Astron. Astrophys.* **234**, 277 (1990)
- Pérez Martínez, M.I., Schröder, K.-P., Cuntz, M.: *Mon. Not. R. Astron. Soc.* **414**, 418 (2011)
- Perryman, M.A.C., Brown, A.G.A., Lebreton, Y., et al.: *Astron. Astrophys.* **331**, 81 (1998)
- Perryman, M.A.C., Lindegren, L., Kovalevsky, J., et al.: *Astron. Astrophys.* **323**, L49 (1997)
- Proctor, R.A.: *Proc. R. Soc. Lond.* **18**, 169 (1869)
- Ramya, P., Reddy, B.E., Lambert, D.L.: *Mon. Not. R. Astron. Soc.* **484**, 125 (2019)
- Redfield, S., Linsky, J.L., Ake, T.B., et al.: *Astrophys. J.* **581**, 626 (2002)
- Richey-Yowell, T.R., Shkolnik, E.L., Schneider, A.C., et al.: *Astrophys. J.* **872**, 17 (2019)
- Rodríguez, D.R., Bessell, M.S., Zuckerman, B., Kastner, J.H.: *Astrophys. J.* **727**, 62 (2011)
- Rodríguez, D.R., Zuckerman, B., Kastner, J.H., et al.: *Astrophys. J.* **774**, 101 (2013)
- Rutten, R.G.M.: *Astron. Astrophys.* **177**, 177 (1987)
- Rutten, R.G.M., Pylyser, E.: *Astron. Astrophys.* **191**, 227 (1988)
- Schröder, K.-P., Mittag, M., Jack, D., Rodríguez Jiménez, A., Schmitt, J.H.M.M.: *Mon. Not. R. Astron. Soc.* **492**, 1110 (2020)
- Schröder, K.-P., Schmitt, J.H.M.M., Mittag, M., Gómez Trejo, V., Jack, D.: *Mon. Not. R. Astron. Soc.* **480**, 2137 (2018)
- Sestito, P., Randich, S., Pallavicini, R.: *Astron. Astrophys.* **426**, 809 (2004)
- Shkolnik, E.L., Barman, T.S.: *Astron. J.* **148**, 64 (2014)
- Simon, T., Drake, S.A.: *Astrophys. J.* **346**, 303 (1989)
- Simon, T., Linsky, J.L., Stencel, R.E.: *Astrophys. J.* **257**, 225 (1982)
- Smith, G.H.: *Astron. J.* **88**, 1775 (1983)
- Smith, G.H.: *Publ. Astron. Soc. Aust.* **35**, 37 (2018)
- Smith, G.H.: *Publ. Astron. Soc. Aust.* **36**, 3 (2019)
- Smith, G.H., Hargrave, M., Eckholm, E.: *Publ. Astron. Soc. Aust.* **34**, 49 (2017)
- Smith, G.H., Redenbaugh, A.K.: *Publ. Astron. Soc. Pac.* **122**, 1303 (2010)
- Soderblom, D.R., Mayor, M.: *Astron. J.* **105**, 226 (1993a)
- Soderblom, D.R., Mayor, M.: *Astrophys. J.* **402**, L5 (1993b)
- Strassmeier, K.G.: *Astron. Astrophys. Suppl. Ser.* **103**, 413 (1994)
- Strassmeier, K.G., Handler, G., Paunzen, E., Rauth, M.: *Astron. Astrophys.* **281**, 855 (1994)
- Sun, M., Jiang, B.W., Zhao, H., Gao, J., Gao, S., Jian, M., Yuan, H.: *Astrophys. J.* **861**, 153 (2018)
- Taberner, H.M., Montes, D., González Hernández, J.I., Ammler-von Eiff, M.: *Astron. Astrophys.* **597**, 33 (2017)
- Taylor, B.J.: *Astron. J.* **134**, 934 (2007)
- Wan, X., Wang, W., Liu, J., Tong, T.: *BMC Med. Res. Methodol.* **14**, 135 (2014)
- Wegner, G.: *Mon. Not. R. Astron. Soc.* **177**, 3 (1976)
- Wenger, M., Ochsenbein, F., Egret, D., et al.: *Astron. Astrophys. Suppl. Ser.* **143**, 9 (2000)
- Wilson, O.C.: *Astrophys. J.* **257**, 179 (1982)